

**Introduction:** Several lines of evidence indicate that the volume of shallow ground ice in the martian high latitudes exceeds the pore volume of the host regolith. Boynton *et al.*<sup>1</sup> found an optimal fit to the Mars Odyssey Gamma Ray Spectrometer (GRS) data at the Phoenix landing site by modeling a buried layer of 50-75% ice by mass (up to 90% ice by volume). Thermal and optical observations of recent impact craters in the northern hemisphere have revealed nearly pure ice<sup>2</sup>. Ice deposits containing only 1-2% soil by volume were excavated by Phoenix<sup>3</sup>.

The leading hypothesis for the origin of this excess ice is that it developed *in situ* by a mechanism analogous to the formation of terrestrial ice lenses and needle ice<sup>4</sup>. Problematically, terrestrial soil-ice segregation is driven by freeze/thaw cycling and the movement of bulk water, neither of which are expected to have occurred in the geologically recent past on Mars. If however ice lens formation is possible at temperatures < 273 K, there are possible implications for the habitability of Mars permafrost, since the same thin films of unfrozen water that lead to ice segregation are used by terrestrial psychrophiles to metabolize and grow down to temperatures of at least 258 K<sup>5</sup>.

**Model:** We have developed a numerical model that applies the physics of pre-melting<sup>6</sup> to track phase partitioning in soil pores and test for conditions under which ice lenses could initiate on Mars. The model balances the thermomolecular forces that arise from intermolecular interactions against gravity and the effective soil overburden pressure. The thermomolecular forces arise because thin films of premelted ice minimize the interfacial free energy between ice and soil particles, leading to strong repulsive forces in the premelted films between ice and soil. It is ultimately this repulsive force that is responsible for frost heave.

The model distinguishes between initiation of an ice lens, which does not involve dissipative forces due to migration of unfrozen water, and the subsequent growth of an ice lens, which is directly limited by the rate of unfrozen H<sub>2</sub>O migration. Here, we rigorously test for lens initiation, and discuss qualitatively the possible subsequent lens growth to macroscopic scale.

In a freezing soil, gravitational forces, and the repulsive thermomolecular force are balanced by the forces transmitted vertically between soil grains.

$$\frac{\partial p_p}{\partial z} = -(1-\phi)(\rho_p - \rho_w)g - \rho_w L_f \frac{T_m - T}{T_m} \frac{\partial(\phi S_i)}{\partial z}$$

Here the first term on the right side of the equation represents the gravitational forces, and the second term the thermomolecular force. The term  $S_i(T)$  denotes the fractional filling of ice pores as a function of temperature,  $T$ , below the freezing point ( $T_m$ ), and is defined for a variety of analog soils<sup>7</sup>. The depth of the ground ice, and the surface temperatures are taken from the historical ground ice model of Zent<sup>8</sup> which provides estimates of ice depth and surface environment over the last 10<sup>7</sup> years.

One simply integrates the force balance equation from the surface down, and if the interparticle pressure  $p_p < 0$  at any depth,  $z$ , then the interparticle forces can unload, and lenses are assumed to initiate.

**Results:** Our results indicate that diurnal cycling in the ice-cemented regolith and resultant pressure gradients in thin films at grain ice interfaces can cause interparticle forces to unload, initiating ice lens formation at temperatures as low as 245 K.

Figures 1-3 show an example from 4.33 Ma before present. In this case, the ice, (depth ~ 7 mm) melts completely each sol, and forces of several bars are generated, leading to lens initiation within 5 - 10 cm of the surface. (The environmental model here assumes that some ice is left at the poles even at relatively high obliquity, in order to buffer atmospheric H<sub>2</sub>O at high levels, which leads to shallow ground ice.). Unfortunately, the ground ice observed by Phoenix must have formed in much more recent times, during which no melting of ground ice can be expected.

Figures 4-6 show a more recent case, from 30 ka bp, where the ground ice is ~ 2 cm deep, and ice temperatures never exceed 240 K. Nonetheless, the very small changes in  $S_i$  over the 30K diurnal temperature swings can produce enough net force to lift up to 30 cm of overburden. Thus, we predict that even it recent times, ice lenses have the potential to at least initiate on Mars. Lens growth however, is dependent on mass transport in very thin films, with permeabilities expected to be extremely low at these temperatures. This may not however, be prohibitive of ice segregation in the long term.

We argue that, unlike Earth, a martian proto-lens may continue its incremental growth from year to year, adding a fraction of a micron each year, until a macroscopic segregated ice lens emerges. No forces arising from premelting physics in the Mars environment would degrade a lens once it initiates, although there may be circumstances where individual solid particles are able to regelate through an ice lens at a speed comparable to its growth rate. These results open the pos-

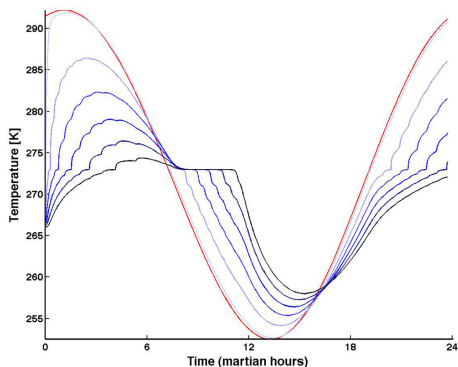


**Figure 1.** 4.33 Ma bp. Soil: Chena Silt. Temperature of the surface layer and the uppermost 6 nodes in the ice.

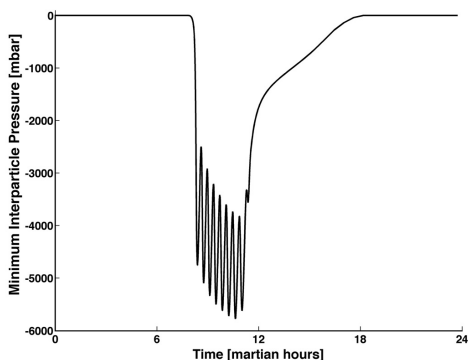


**Figure 2.** 4.33 Ma bp. Soil: Chena Silt. The minimum interparticle pressure in the column, over a sol.

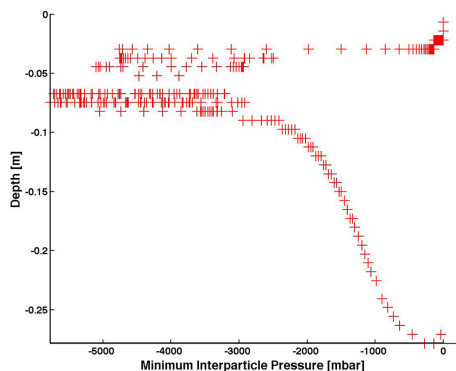


**Figure 3.** 4.33 Ma bp. Soil: Chena Silt. The depth of the minimum interparticle pressure.

sibility that *in situ* ice segregation, and slow, multi-annual accumulation of segregated ice may account for much of the observed excess ice.

**References:** [1] Boynton W. V. *et al.*, *Science*, **297**, 81-85, (2002). [2] Byrne, S., *et al.*, *Science*, **325**, 1674-1676, (2009). [3] Smith, P. H. *et al.*, *Science*, **325**, 58 – 61, (2009). [4] Mellon, M. T. *et al.*, *JGR*, **114**, E00E07, (2009). [5] Rivkina, E. M. *et al.*, *Appl. Envi-*

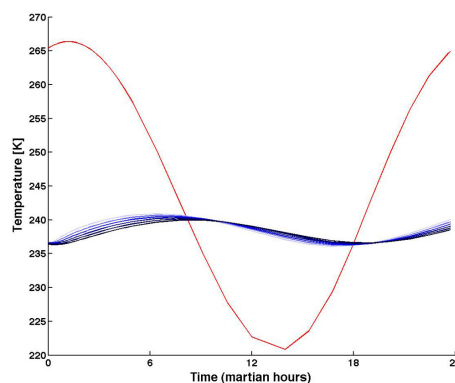


**Figure 4.** Chena Silt -30 ka bp. Same as Figure 1

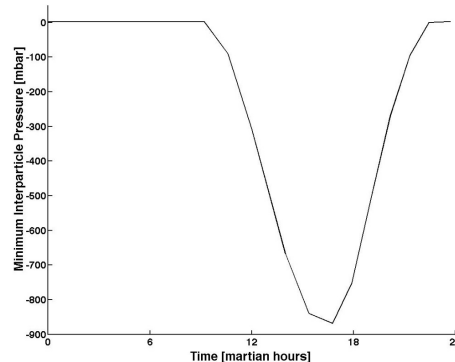


**Figure 5.** Chena Silt -30 ka bp. Same as Figure 2.

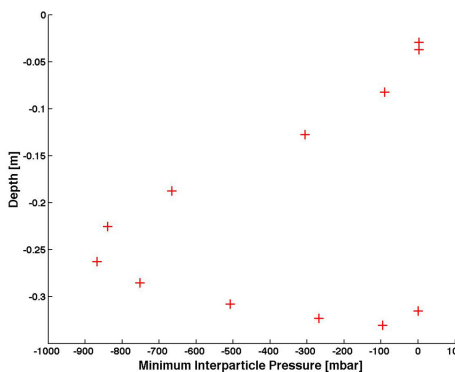


**Figure 6** Chena Silt -30 ka bp. Same as Figure 3.

*ron. Microbio.*, **66**, 3230-3233, (2000). [6] Rempel, A. W., *et al.*, *Phys. Rev. Lett.*, **87**, 088501, (2001). [7] Andersland, O. B., and B. Ladanyi, *An Introduction to Frozen Ground Engineering*, 363 pp., CRC Press, Boca Raton, FL, (2004) [8] Zent, A. P., *Icarus*, **196**, 385–408, (2008)